

Dendritic Spines as Space Charge Limited Devices

Abstract

Gap junctions are essential for the synchronization of neural oscillations among populations of neurons. These neural oscillations are correlated with various behavioral states in waking and sleep, but their role in cognitive processes and their underlying mechanisms are not well understood. In particular, it is yet unknown why the auditory steady state response (ASSR) is enhanced at frequencies of about 20 & 40 Hz.

Here we suggest treating electrically coupled dendritic spines as space charged limited (SCL) devices. The main conduction mechanism in these devices is electrical drift rather than diffusion. The frequency response of two dendritic spines, electrically coupled by a gap junction, is characterized using an existing small-signal model for the frequency response of a SCL device. We reconstruct the human ASSR curve as a linear combination of the frequency responses of three charge carriers. These charge carriers are suggested to be potassium and sodium ions drifting through the gap junction, and potassium ions drifting through the spine neck. The suggested passage times for these charge carriers are 23.2, 30.8 and 46.7 ms. The resulting peak at 40 Hz is robust to 200% variations in the gap junction conduction, as required in a noisy physiological environment and in accordance with experimental findings. The suggested model yields several experimental predictions, which shall enable its validation.

1. Introduction

1.1 The auditory steady state response

The auditory steady-state response (ASSR) is a remarkable neurophysiological phenomenon. Rhythmical auditory stimuli at various frequencies elicit a time locked steady-state neural response, which peaks in amplitude for a stimulus frequency of about 40 Hz [1]. ASSRs can be elicited by a variety of periodic stimuli such as clicks, pure tones, and amplitude or frequency modulation of continuous sounds [2]. They are astonishingly well time-locked to the eliciting stimulus [3].

The ASSR originates from multiple generators, including the primary and secondary auditory cortices [4]. Since its identification in 1981 [5], the cause of the enhanced response for ~40 Hz stimulation has been intensely debated [1,3,5-7]. It has been suggested to reflect a resonance phenomenon indicating the preferential working frequency of the auditory network [1,6-7], but its underlying mechanisms are unknown.

Ross et al. [8] measured the MEG ASSR of eight human subjects to an AM stimulus in the 10-100 Hz range. They found a clear phase-locking to the first and second harmonics of the given stimulus, peaking at ~22 and 40 Hz. This curve (figure 1) was obtained by normalizing the ASSRs of eight subjects according to their amplitude at 40 Hz. The ~20 Hz peak was higher than the 40 Hz peak in two of the eight subjects. The 40 Hz peak was conserved in frequency among all eight subjects, whereas the ~20 Hz peak exhibited inter-individual variations of up to ~10 Hz. A third peak at ~80 Hz was much weaker yet statistically significant.

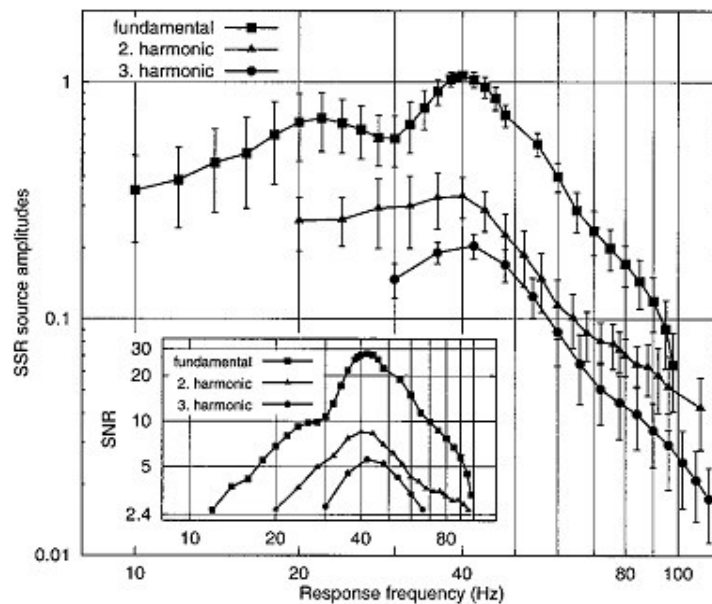


Figure 1 - Grand-averaged ASSR at the stimulus frequency, and its first and second harmonics, normalized by 40 Hz ASSR. Copied from [8].

Similar peaks at ~20, ~40 and ~80 Hz were reported later by Artieda et al. [6]. Moreover, the frequency spectrum of subthreshold oscillations in a slice of the thalamic nucleus of Zebra Finch birds (involved in their song system) revealed similar three peaks, at cruder spectral resolution [9]. In the visual modality, the neural response to flickering stimuli at 1-100 Hz exhibited peaks at ~10, ~20, ~40, and ~80 Hz, in both cats [10] and humans [11]. Thus, the enhanced sensitivity to ~20, ~40 and ~80 Hz stimuli seems to be multimodal [12]. Its similarity in different vertebrates is congruent with the similar spectra of neural oscillations among vertebrates [13].

1.2 The neural origin of ASSR

Magnetoencephalography (MEG) is used to measure the tangential magnetic fields formed along the scalp. These fields are proportional to the net radial component of the electrical currents in the head. The dominant contribution to MEG signal stems from post-synaptic currents in the apical dendrites of cortical pyramidal neurons [14]. This is due to the radial orientation of apical dendrites [14] and the significant dipolar component of post-synaptic currents [14-15]. Human pyramidal dendrites are densely populated with dendritic spines [16], which account for up to half of the dendritic membrane area [17]. As the electrical function of dendritic spines is yet unclear [17-18], it has been recently suggested that they filter post-synaptic potentials [18]. This is congruent with an earlier finding in electric fish [19], that spiny pyramidal neurons are selectively sensitive to ~5 Hz stimuli whereas non-spiny neurons are non-selective.

In non-pyramidal neurons, the dendritic spines of neighboring neurons are sometimes electrically coupled by a gap junction [20-21]. The neural role of gap junctions is yet unclear [22-23]. Misexpression of a neural gap junction protein named Cx36 impairs neural oscillations in the ~30-70 Hz range, while sparing neural oscillations in other frequency bands [20-21,24-28]. This finding along with others support a role for gap junctions in the synchronization of neural oscillations [22-23,27,29-30].

1.3 Space-charge-limited devices

This work attempts to harness an existing small signal model [31-33], describing the frequency response of a one-dimensional space-charge-limited (SCL) device, to reconstruct the ASSR curve measured at [8]. In SCL devices the dominant conductance mechanism is electrical drift and not diffusion. Consequently the characteristic relaxation time τ is dependent on the passage time T_a of a charge carrier through the device ($\tau \approx 1.38 T_a$). This passage time can be calculated using the following approximate equation:

$$(1) \quad T_a = \frac{d^2}{V_{app} \cdot \mu}$$

Where d is the device length, V_{app} is the applied DC voltage and μ the charge carrier mobility. We first empirically determined the passage times that yield a frequency response similar to that measured in [8]. As demonstrated in section 2.2 below, this response can be reconstructed using three charge carriers with passage times of 23.2, 30.8 and 46.7 ms. Given the typical amplitudes of sub-threshold oscillations in membrane potential and the mobilities of the main intracellular charge carriers (mainly K^+ ions), we can thereby bound the typical length of the desired neural structure to ~ 1 -3 microns.

Dendritic spines fit this length scale, and were found to exhibit much slower diffusion rates than dendrites [34]. We thus suggest a simplistic model treating dendritic spines as SCL devices.

2. Model

2.1 Outline

Let two dendritic spines be electrically coupled by a single gap junction. Each spine belongs to the apical dendrite of a pyramidal neuron. Both spines and shafts are assumed to be held at the same resting potential. At $t=0$ one of the spines (A) undergoes a single EPSP, taken as an instantaneous change in local sodium and potassium concentrations at its PSD. Consequently, sodium ions drift from spine A to spine B through the gap junction, while potassium ions drift in the other direction. In addition, potassium ions drift from the dendritic shaft towards the head of spine A, via the spine neck. We treat this movement as having two SCL devices connected in parallel: one device corresponding to drift through the gap junction, and the other corresponding to the drift through the spine head and neck. The lengths of these devices are illustrated in figure 2:

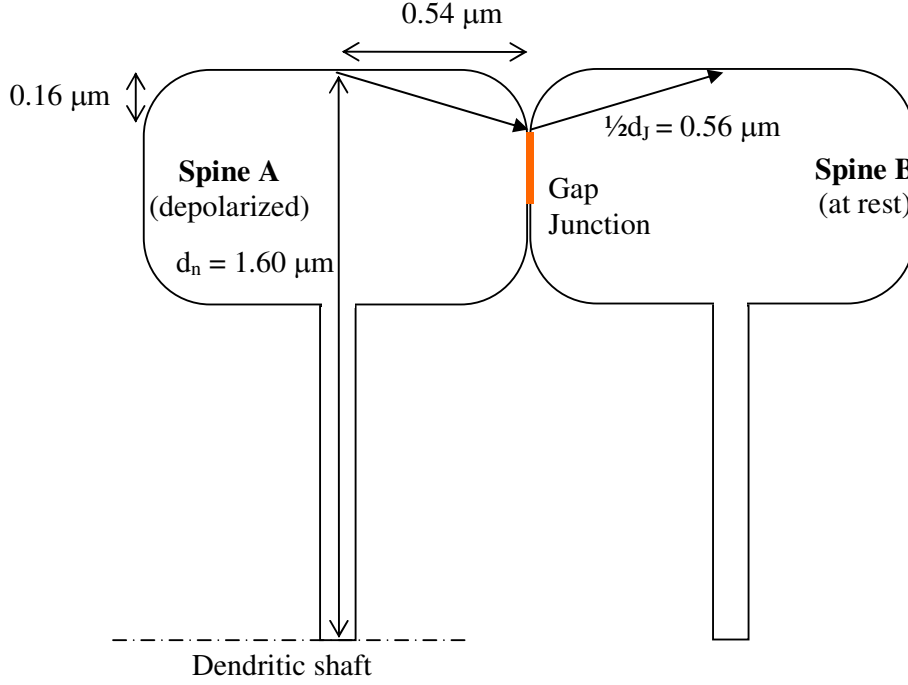


Figure 2 – Electrically coupled dendritic spines of human pyramidal neurons as SCL devices (Scale 5000:1).

The measurements of the dendritic spines dimensions are taken from [35] whereas the 0.16 μm figure is pure guess, as elaborated below. Using equation (1) we calculated the potential gradients that will yield the required passage times. First, for the potassium ions flowing through the gap junction:

$$(2) \quad V_{GJ-K^+} = \frac{d_J^2}{T_{a-K^+} \cdot \mu_{K^+}} = \frac{(1.08 \cdot 10^{-4} \text{ cm})^2}{2.32 \cdot 10^{-2} \text{ sec} \cdot 7.92 \cdot 10^{-4} \text{ cm}^2 / V \cdot \text{sec}} = 0.635_{mV}$$

Similarly, for the sodium ions flowing through the gap junction in the other direction:

$$(3) \quad V_{GJ-Na^+} = \frac{d_J^2}{T_{a-Na^+} \cdot \mu_{Na^+}} = \frac{(1.08 \cdot 10^{-4} \text{ cm})^2}{3.08 \cdot 10^{-2} \text{ sec} \cdot 5.39 \cdot 10^{-4} \text{ cm}^2 / V \cdot \text{sec}} = 0.70_{mV}$$

Finally, for the potassium ions flowing up the spine neck and head:

$$(4) \quad V_{neck-K^+} = \frac{d_n^2}{T_{a-K^+} \cdot \mu_{K^+}} = \frac{(1.6 \cdot 10^{-4} \text{ cm})^2}{4.67 \cdot 10^{-2} \text{ sec} \cdot 7.92 \cdot 10^{-4} \text{ cm}^2 / V \cdot \text{sec}} = 0.69_{mV}$$

We got different voltages for the K^+ ions through the gap junction and the spine neck. This result does not conform to our assumption that both dendrites and spines initially shared the same resting potential. This discrepancy may be resolved if we take the length of the first device to be 1.13 μm rather than 1.08 μm. This assumption conforms to the fact that the gap junction is only spread across a disc of ~0.2 microns diameter [36]. If we allow the center of

this disc to reside about $0.26 \mu\text{m}$ below the top of the spine head, as illustrated in figure 2 above, we get an effective device of length $1.13 \mu\text{m}$. The voltages through the gap junction for the K^+ and Na^+ ions will then be 0.69 and 0.76 mV, respectively. These voltages are similar to those measured for a single EPSP in the dendritic spines of mice: 0.86 ± 0.07 mV [37].

2.2 ASSR reconstruction

The passage times of the three charge carriers were so chosen to best match the ASSR curve measured at [8]. Specifically, each charge carrier contributes the following term to the small-signal susceptance per unit area:

$$(5) \quad B(g, \theta) = \frac{g\theta^3}{6} \cdot \frac{\theta^2/2 + \cos\theta - 1}{(\theta - \sin\theta)^2 + (\theta^2/2 + \cos\theta - 1)^2}$$

where $g \triangleq \frac{3\varepsilon^2}{\mu J_0 T_a^3}$; $\theta \triangleq \omega T_a$ and J_0 is the DC current density. We subtract the asymptotic susceptance at high frequencies ($g\theta/3$) to obtain an all-negative susceptance, reflecting a capacitative device [31-33].

Taking the passage times T_a of the three charge carriers to be 23.2 , 30.8 and 46.7 ms, with conductance (g) ratios of $1 : -1.5 : 3.2$ in favor of the fastest charge carrier ($T_a = 23.2$ ms) yield the normalized susceptance curve plotted in figure 3.

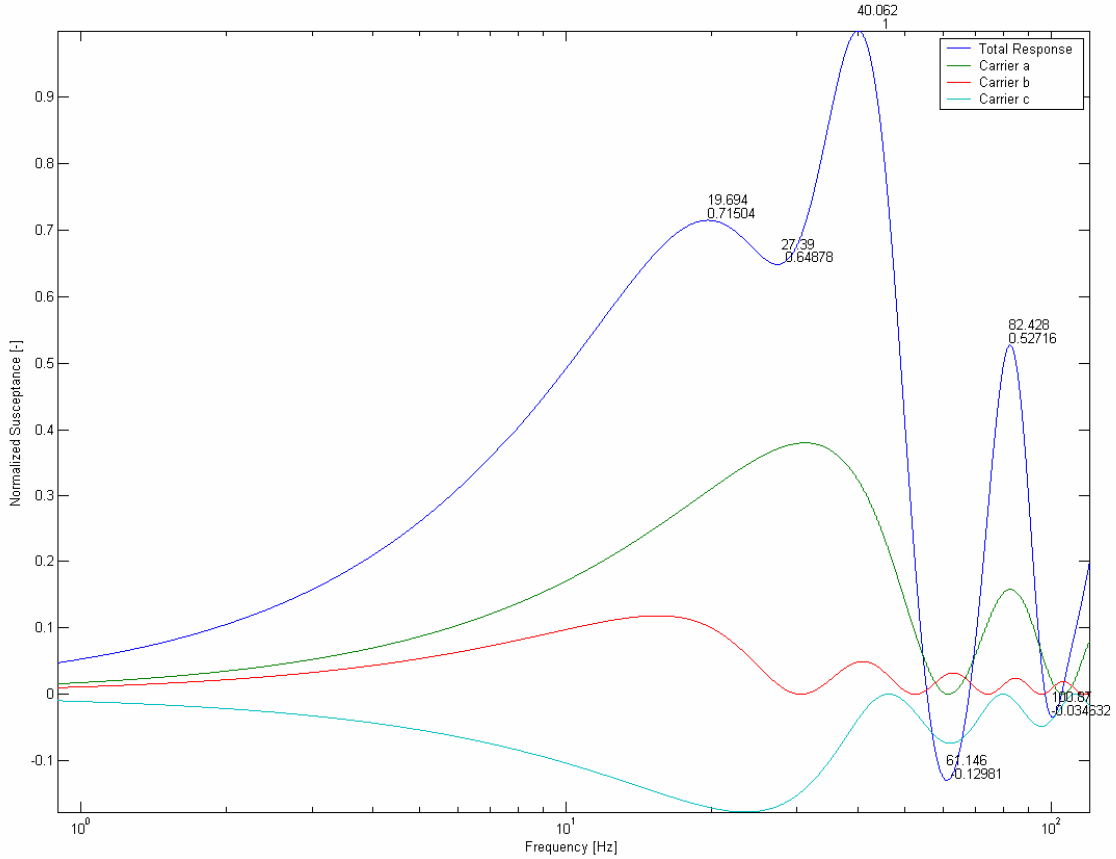


Figure 3 – Reconstruction of the ASSR curve from [8] using three charge carriers

Note that the secondary charge carrier, with $T_a=30.8$ ms, partially cancels out the contributions of the primary and tertiary charge carriers. In our model this corresponds to Na^+ ions drifting out of the head of spine A while K^+ ions drift in.

The secondary peak at ~ 20 Hz is 72% the height of the ~ 40 Hz peak, versus $67\pm 22\%$ measured in [8]. The local trough at ~ 27 Hz is 65% the height of the ~ 40 Hz peak, versus $57\pm 15\%$ measured in [8]. The ~ 80 Hz peak is significantly higher than that measured in [8].

The MEG ASSR reflects the overall contribution of an ensemble of dendritic spines, of various shapes and synaptic strengths, over millions of apical dendrites. Thus the average dimensions of dendritic spines, as measured in [35], are expressed in the ASSR curve, via eq. (1).

2.3 Robustness

The proposed frequency response is dependent on the typical passage time of each charge carrier, and the conductance ratios between them. Let's probe the robustness of the proposed response to variations in these parameters. First, let's see how the frequency response varies as we double or half the conductance of each charge carrier (figure 4).

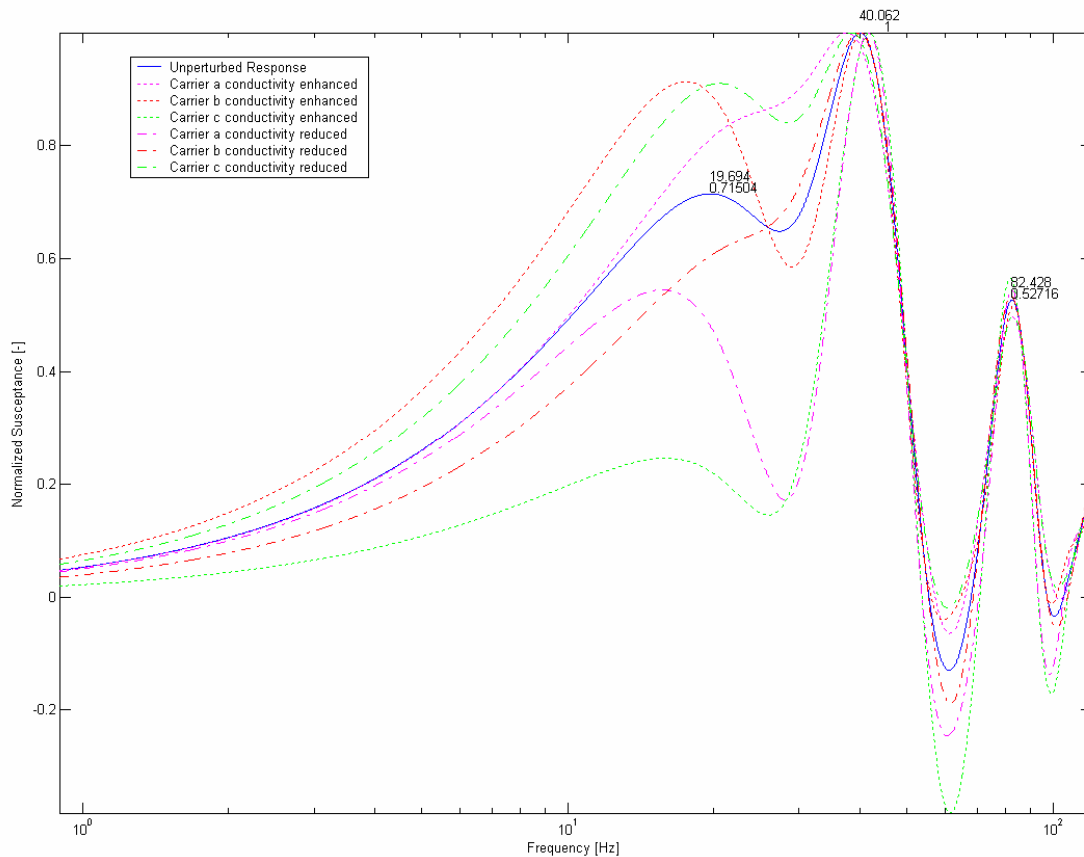


Figure 4 –Robustness of the proposed solution to 200% variations in the conductance of each charge carrier

We see that the ~ 40 Hz peak is conserved under 200% variations in conductivity. The ~ 20 Hz peak is conserved in frequency and amplitude to a lesser degree. Considering the developmental variations in gap junction conductance [36], this variation is compatible with the inter-individual differences found in [8].

There is also lesser robustness to variations in the passage times of each of the three charge carriers. Figure 5 illustrates the resulting variations in frequency response as each of the passage times is multiplied or divided by 1.25:

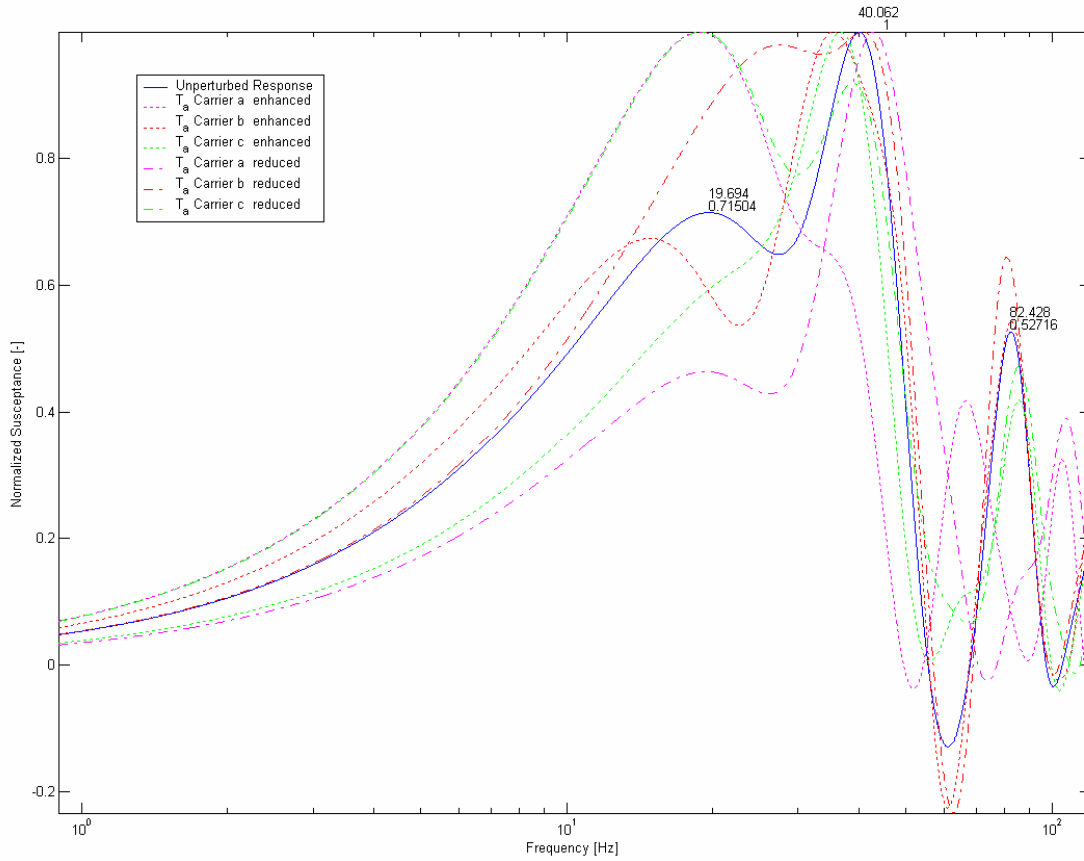


Figure 5 – Robustness of the proposed solution to 25% variations in the passage time of each charge carrier

According to eq. (1), the typical passage time of each ion is in itself a function of its mobility, the device length and the voltage upon it. The ion mobility is spatially uniform, at least according to the model assumptions (see next section). We expect the variance in spine length and diameter to average out across an ensemble of dendritic spines. This averaging holds both for a single pyramidal neuron, populated with thousands of spines, and for the MEG signal which stems from the synchronized activity of millions of neurons [14-15]. However, the voltage upon the device decays as time elapses from the EPSP initiation. The voltage is expected to vary uniformly over both devices, thus the voltage variation should induce a corresponding variation in the typical passage times of a given ion through both devices. For a slow voltage decay (100 ms or more [38]), we have to convolve the voltage decay with the frequency response for a fixed voltage. We expect a broadening of the frequency response peaks which shall be proportional to the voltage variation:

$$(6) \quad \frac{\delta f_{resonance}}{f_{resonance}} \propto \frac{\delta V_{app}}{V_{app}}$$

2.4 Assumptions

The model we use is based on the following set of assumptions:

2.4.1. The diffusion current is negligible with respect to the drift current

The key assumption in treating a device as space-charge-limited is that electrical drift is the main conduction mechanism through it. In the case of dendritic spines, this assumption is based on the finding that the rate of diffusion from the spine head to the dendritic shaft is considerably slower (up to 500 fold) than that measured in the dendrite itself [34]. Let's assume that diffusion through the dendritic spine is α times slower than in plain cytosol, and find the voltage difference for which the diffusion current is negligible with respect to the drift current.

Let p be the K^+ concentration in the device. Expressing the drift and diffusion currents:

$$(7) \quad J_{Drift} = q\mu Ep; \quad J_{Diffusion} = q \frac{D_{aq}}{\alpha} \cdot \frac{dp}{dz}$$

Demanding the diffusion current to be negligible with respect to the drift current, and plugging the Einstein relation:

$$(8) \quad J_{Drift} = q^2 \frac{D_{aq}}{k_B T} \cdot Ep \gg q \frac{D_{aq}}{\alpha} \cdot \frac{dp}{dz} = J_{Diffusion}$$

Replacing the electric field with its mean value over the entire device $E \approx \frac{V_{app}}{d}$:

$$(9) \quad q^2 \frac{D_{aq}}{k_B T} \cdot \frac{V_{app}}{d} \cdot p \gg q \frac{D_{aq}}{\alpha} \cdot \frac{dp}{dz}$$

Similarly, replacing the local concentration gradient with its mean value over the entire device $\frac{dp}{dz} \approx \frac{\Delta p}{d}$:

$$(10) \quad q^2 \frac{D_{aq}}{k_B T} \cdot \frac{V_{app}}{d} \cdot p \gg q \frac{D_{aq}}{\alpha} \cdot \frac{\Delta p}{d}$$

Thus our demand simplifies to:

$$(11) \quad V_{app} \gg \frac{k_B T}{q\alpha} \cdot \frac{\Delta p}{p}$$

A PSP is expected to moderately affect the local potassium concentration with respect to its dendritic concentration $\frac{\Delta p}{p} < 1$:

$$(12) \quad V_{app} \gg \frac{k_B T}{q\alpha} \approx \frac{27mV}{\alpha}$$

Specifically for $\alpha = 100$ we obtain:

$$(13) \quad V_{app} \gg 0.27mV$$

Thus, already for rather small voltages, the drift current is the dominant conduction mechanism for potassium ions in dendritic spines. The same treatment holds for sodium ions, with the upper bound $\frac{\Delta p}{p} < 1$ becoming tight for sodium ions [38]. Note that the assumption that

diffusion is significantly slower in dendritic spines than in the cytosol is essential – if $\alpha = 1$ than the diffusion current cannot be neglected for any sub-threshold voltage.

Thus we found that electrical drift is the dominant conduction mechanism for the sub-threshold voltages treated in this work (see eqs. 2-4). The diffusion current cannot be neglected in the intercellular solution and in other neural regions.

2.4.2. Inter-ionic interactions are neglected

This analysis does not treat the injection mechanism of ions into the device. Nor do we take into account direct interactions between the ions in the device.

2.4.3. Diffusion model

For the diffusion model to be valid, the characteristic time between consecutive scatterings of ions with water molecules has to be much shorter than the typical timescale of variations in the electric field. As we treat an electric field varying at frequencies lower than 1 KHz, this condition is held to be valid.

2.4.4. Linear device response

The decomposition of the input voltage into a large DC signal and a small AC signal is based on the linearity of the device (for which a harmonic signal is an eigensignal of the system). Accordingly, the electrical transmission through cortical gap junctions is linear, at least up to intercellular voltages of up to ± 40 mV [39-40]. Specifically, both types of neural gap junction proteins - connexin Cx36 [40] and pannexin Px1 and Px2 [41] – respond linearly to voltages of up to ± 40 mV.

2.4.5. Neglecting higher harmonics

As usual in small signal analysis, we use the adiabatic approximation according to which higher order harmonics are averaged out during the timescale of the slower small signal variations. Thus these terms are neglected in the total device response.

2.4.6. Frequency independent mobility

For the simplicity of our analysis, we assume that the ionic mobilities through the device are independent of the frequency and magnitude of the electrical field. We may expand the analysis to take into account a frequency-dependent mobility, as done for instance in [32], but for the low frequency range probed in this work this extension is assumed to be unnecessary.

2.4.7. The ions entrance velocities are neglected

For the simplicity of our analysis, we neglect the velocity of the ions at the entrance(s) to our device(s). The analysis may be extended to take this parameter into account as well.

2.4.8. Spatially uniform mobilities and dielectric constant

This analysis is based on the assumption that the ion mobilities and dielectric constant are uniform along the entire device(s). Specifically, we take the ion mobilities to be identical for the dendritic spine head and neck, and neglect the variation in mobility along the gap junction [42]. As the gap junction length is negligible with respect to the head diameter of the spine, this assumption is not expected to significantly affect the analysis results.

3. Discussion

3.1 Reservations

Currently there are several deficiencies in the simplistic model suggested here.

First, the model is based on the common electrical coupling between dendritic spines in neighboring pyramidal apical dendrites. Unfortunately we could not find an estimate for the propensity of such coupling, possibly since pannexin gap junctions, which couple pyramidal neurons, were only identified in humans by 2003 [41]. Examples for the synchronization of neural oscillations via electrical coupling between dendritic spine heads for **non-pyramidal** neurons may be found at [20-21].

Moreover, we assumed that diffusion is uniformly impeded across the dendritic spine – head and neck alike. If diffusion is locally obstructed in the spine neck, we cannot treat the spine head as a SCL device as done here. The experimental evidence we have traced [18,34,38] does not determine whether diffusion is obstructed only in the spine neck. Lateral diffusion of AMPA receptors along the dendritic membrane has been shown to be slowed in neck-less dendritic spines as well as in spines with necks [43], suggesting that this lateral diffusion is impeded in the spine head as well. Further experimental findings are required in order to resolve this matter.

In addition, we do not have any direct experimental finding linking the ~20 Hz peak in human ASSR with the suggested drift of K^+ ions from the dendrite to the spine head. Nevertheless, the fact that misexpression of connexin-36 gap junctions impairs neural oscillations only in the ~30-70 Hz range [24-28] is congruent with the assumption that the ~20 Hz peak does not reflect the flow of ions through the gap junction.

As noted above (section 2.3), one has to convolve the suggested frequency response for a fixed voltage with the temporal profile of voltage decay in the dendritic spine head following a EPSP. Exchanging the voltages found in eqs. (2-4) with realistic voltage intervals will be expressed as a broadening of the frequency response peaks, which shall be proportional to the voltage variation, in accordance with eq. (6).

In this work we took into account only three charge carriers, as these sufficed to reconstruct the frequency response measured in [8]. For the completeness of our model we have to take into account a fourth charge carrier, namely the drift of sodium ions from the dendritic spine head towards the dendritic shaft. The contribution of this component is expected to be rather minor compared to those of the three charge carriers we considered. We disregarded the contribution of chloride ions for the following reasons:

- A. An influx of chloride ions, from the extracellular solution into the spine, is unlikely due to relative absence of inhibitory Cl^- channels on dendritic spines.
- B. The intracellular chloride concentration is rather low with respect to that of potassium.
- C. The mobility of potassium ions is similar to that of sodium ions, suggesting that any contribution of Cl^- current will be overshadowed by that of K^+ ions [44].

The intracellular concentration of calcium ions, even in dendritic spines, is too low to attribute a significant direct influence on the measured frequency response. Other charge carriers may be neglected, for the present accuracy level of our model.

Finally, the measurements we used of dendritic spines lengths were taken from human **basal** dendrites [35]. We assume these values are also valid for dendritic spines in **apical** dendrites, but we could not find any studies confirming this assumption.

3.2 Predictions & conclusions

Several experimental predictions can be produced from the suggested model, which shall enable its validation. A key prediction is that the ratio between the primary and secondary ASSR peaks approximately equals the squared ratio between the spine length (head + neck) and its diameter. This prediction is compatible with the fact that cognitive dysfunctions associated with disruptions to the spectra of neural oscillations [45], such as schizophrenia and epilepsy, are also associated with distortions in the shapes and sizes of dendritic spines [46]. Yet this correlation does not necessarily imply a direct causal link between the two – possibly defects in the mechanisms that are actually responsible for neural oscillations lead to dendritic spine deformation.

Hence we may compare the dimensional ratio (length/diameter) of dendritic spines in different species, to the frequency ratio of neural oscillations (primary/secondary ASSR peak frequencies) in the same species. We calculated the dimensional ratios for the dendritic spines of humans and mice, as measured in [35]. While human dendritic spines are much larger than those of mice, the ratio between their height (head + neck) and width is highly conserved: 1.481 ± 0.019 in humans and 1.488 ± 0.025 in mice. According to our model, this similarity conforms to the similar patterns of neural oscillations for mammals [13]. We expect this similarity to be conserved in other mammals as well. The model also enables a comparison with species exhibiting entirely different spectra of neural oscillations, once the dimensions of their dendritic spines are measured.

The amplitude ~40 Hz ASSR increases with age, especially during puberty [2], with no shift in the frequencies of peak ASSR around ~20 and ~40 Hz [12]. Therefore we may predict that the dimensional ratio (length/diameter) of human dendritic spines does not significantly vary with age. Three possible explanations may be given for the developmental increase in ~40 Hz ASSR: an increase in spine density, an increase in the fraction of electrically coupled spines, or an increase in the conductance of gap junctions between dendritic spines.

It has been previously suggested, that gap junctions are required for the local synchronization of neural oscillations, whereas distant cortical areas are synchronized by inhibitory interneurons [47]. Similarly we may speculate, that the model suggested here deals with the **local** synchronization of neural oscillations, whereas long-distance coordination may be modeled by more intricate computational models [48]. In this sense this work aims at complementing, rather than replacing, these prior works.

Conclusively, we suggest that electrically coupled dendritic spines in cortical pyramidal neurons play an essential role in the synchronization of neural oscillations. Based on an existing model for the frequency response of a space-charge-limited device, we suggest a reconstruction of the human auditory steady state response, a phenomenon that has no entire explanation to date. Despite its simplicity, the proposed model successfully reproduces the grand-averaged response as well as the inter-individual differences measured at [8], as an outcome of variations in the average coupling strength between the spines. Several experimental predictions are drawn from the model, which will enable its validation.

4. Bibliography

- [1] Pastor M., Artieda J., Arbizu J., Marti-Climent J., Peñuelas I., Masdeu J., '**Activation of Human Cerebral and Cerebellar Cortex by Auditory Stimulation at 40 Hz**', J. Neurosci., Dec 2002; 22: 10501 - 10506.
<http://www.jneurosci.org/cgi/content/abstract/22/23/10501>
- [2] Rojas D., Maharajh K., Teale P., Kleman MR, Benkers T., Carlson J., Reite M., '**Development of the 40 Hz steady state auditory evoked magnetic field from ages 5 to 52**', Clin. Neurophys., 117 (1), January 2006, pp. 110-117
<http://dx.doi.org/10.1016/j.clinph.2005.08.032>
- [3] Ross B., Herdman A.T., and Pantev C., '**Stimulus Induced Desynchronization of Human Auditory 40-Hz Steady-State Responses**', J. Neurophysiol. 94 , Dec 2005, pp. 4082 - 4093.
<http://dx.doi.org/10.1152/jn.00469.2005>
- [4] Herdman AT, Lins O, Van Roon P, Stapells DR, Scherg M, Picton TW., '**Intracerebral Sources of Human Auditory Steady-State Responses**', Brain Topogr. 2002 Winter;15(2):69-86
<http://dx.doi.org/10.1023/A:1021470822922>
- [5] Galambos R., Makeig S., and Talmachoff P.J., '**A 40-Hz auditory potential recorded from the human scalp**', PNAS 78(4), 1981 Apr, pp. 2643-2647.
<http://www.pnas.org/cgi/content/abstract/78/4/2643>
- [6] Artieda J., Valencia M., Alegre M., Olaziregi O., Urrestarazu E. and Iriarte J., '**Potentials evoked by chirp-modulated tones: a new technique to evaluate oscillatory activity in the auditory pathway**', Clinical Neurophysiology, 115(3), March 2004, pp. 699-709
<http://dx.doi.org/10.1016/j.clinph.2003.10.021>
- [7] Santarelli R., Maurizi M., Conti G., Ottaviani F., Paludetti G., Pettorossi V.E., '**Generation of human auditory steady-state responses (SSRs). II: Addition of responses to individual stimuli**', Hearing Research, 83 (1-2), March 1995, pp. 9-18
[http://dx.doi.org/10.1016/0378-5955\(94\)00185-S](http://dx.doi.org/10.1016/0378-5955(94)00185-S)
- [8] Ross B., Borgmann C., Draganova R., Roberts L.E., Pantev C., '**A high-precision magnetoencephalographic study of human auditory steady-state responses to amplitude-modulated tones**', J. Acoust Soc. Am. 108(2), 2000 Aug, pp. 679-91
<http://dx.doi.org/10.1121/1.429600>
- [9] Luo M, Perkel D.J., '**A GABAergic, Strongly Inhibitory Projection to a Thalamic Nucleus in the Zebra Finch Song System**', J. Neurosci., 19, August 1999, pp. 6700 - 6711.
<http://www.jneurosci.org/cgi/content/abstract/19/15/6700>
- [10] Rager G., Singer W., '**The response of cat visual cortex to flicker stimuli of variable frequency** ', Eur. J. Neurosci, 10 (5), May 1998, pp.1856-1877
<http://dx.doi.org/10.1046/j.1460-9568.1998.00197.x>
- [11] Herrmann C.S., '**Human EEG responses to 1–100 Hz flicker: resonance phenomena in visual cortex and their potential correlation to cognitive phenomena**', Exp. Brain Res., 137 (3 – 4), Apr 2001, pp. 346 - 353,
<http://dx.doi.org/10.1007/s002210100682>
- [12] Golgher L., '**Synchronous Neural Oscillations and Motor Vehicle Vibrations - A Preliminary Literature Survey**', Weizmann Institute of Science, Rehovot, June 2006.
<http://techst02.technion.ac.il/~sheket/p/4.pdf>
- [13] Llinás R.R., Steriade M., '**Bursting of Thalamic Neurons and States of Vigilance**', J Neurophysiol, 95 (6), June 2006, pp.3297 - 3308.
<http://dx.doi.org/10.1152/jn.00166.2006>
- [14] Okada Y, Lauritzen M, Nicholson C., '**MEG source models and physiology**', Phys Med Biol. 1987 Jan;32(1):43-51
<http://dx.doi.org/10.1088/0031-9155/32/1/007>

- [15] Hämäläinen M., Hari R., Ilmoniemi R.J., Knuutila J., Lounasmaa O.V., '**Magnetoencephalography— theory, instrumentation, and applications to noninvasive studies of the working human brain**', Rev. Mod. Phys. 65, 413 - 497 (1993)
<http://dx.doi.org/10.1103/RevModPhys.65.413>
- [16] Elston GN, Benavides-Piccione R, DeFelipe J., '**The pyramidal cell in cognition: a comparative study in human and monkey**', J Neurosci. 2001 Sep 1;21(17):RC163
<http://www.jneurosci.org/cgi/content/abstract/21/17/RC163>
- [17] Tsay D, Yuste R., '**On the electrical function of dendritic spines**', Trends Neurosci. 2004 Feb;27(2):77-83
<http://dx.doi.org/10.1016/j.tins.2003.11.008>
- [18] Araya R, Jiang J, Eiselthal KB, Yuste R., '**The spine neck filters membrane potentials**', PNAS 2006 Nov 21;103(47):17961-6
<http://dx.doi.org/10.1073/pnas.0608755103>
- [19] Rose G.J., Call S.J., '**Temporal filtering properties of midbrain neurons in an electric fish: implications for the function of dendritic spines**', J. Neurosci., Mar 1993; 13: 1178 - 1189.
<http://www.jneurosci.org/cgi/content/abstract/13/3/1178>
- [20] Szabadics J, Lorincz A, Tamas G., ' **β and γ Frequency Synchronization by Dendritic GABAergic Synapses and Gap Junctions in a Network of Cortical Interneurons**', J Neurosci. 2001 Aug 1;21(15):5824-31.
<http://www.jneurosci.org/cgi/content/abstract/21/15/5824>
- [21] De Zeeuw CI, Chorev E, Devor A, Manor Y, Van Der Giessen RS, De Jeu MT, Hoogenraad CC, Bijman J, Ruigrok TJ, French P, Jaarsma D, Kistler WM, Meier C, Petrasch-Parwez E, Dermietzel R, Sohl G, Gueldenagel M, Willecke K, Yarom Y., '**Deformation of network connectivity in the inferior olive of connexin 36-deficient mice is compensated by morphological and electrophysiological changes at the single neuron level**', J Neurosci. 2003 Jun 1;23(11):4700-11
<http://www.jneurosci.org/cgi/content/abstract/23/11/4700>
- [22] Amitai Y., Gibson J.R., Beierlein M., Patrick S.L., Ho A.M., Connors B.W., Golomb D., '**The spatial dimensions of electrically coupled networks of interneurons in the neocortex**', J Neurosci. 2002 May 15;22(10):4142-52
<http://www.jneurosci.org/cgi/content/abstract/22/10/4142>
- [23] Weickert S., '**On the search for neuronal gap junctions: quantitative analysis of connexin and pannexin gene expression in electrically coupled areas of the brain**', *Dissertation*. International Graduate School of Neuroscience, Ruhr-University Bochum 2004
<http://www-brs.ub.ruhr-uni-bochum.de/netahtml/HSS/Diss/WeickertSvenja/diss.pdf>
- [24] Connors B.W., Long M.A., '**Electrical synapses in the mammalian brain**', Annu Rev Neurosci. 2004;27:393-418
<http://dx.doi.org/10.1146/annurev.neuro.26.041002.131128>
- [25] Bennett M.V., Zukin R.S., '**Electrical coupling and neuronal synchronization in the Mammalian brain**', Neuron. 2004 Feb 19;41(4):495-511
[http://dx.doi.org/10.1016/S0896-6273\(04\)00043-1](http://dx.doi.org/10.1016/S0896-6273(04)00043-1)
- [26] Deans M.R., Gibson J.R., Sellitto C., Connors B.W., Paul D.L., '**Synchronous activity of inhibitory networks in neocortex requires electrical synapses containing connexin36**', Neuron 2001 Aug 16;31(3):477-85
[http://dx.doi.org/10.1016/S0896-6273\(01\)00373-7](http://dx.doi.org/10.1016/S0896-6273(01)00373-7)
- [27] Buhl DL, Harris KD, Hormuzdi SG, Monyer H, Buzsaki G., '**Selective Impairment of Hippocampal Gamma Oscillations in Connexin-36 Knock-Out Mouse In Vivo**', J. Neurosci., Feb 2003; 23: 1013 - 1018
<http://www.jneurosci.org/cgi/content/abstract/23/3/1013>
- [28] Hormuzdi S.G., Pais I., LeBeau F.E., Towers S.K., Rozov A., Buhl E.H., Whittington M.A., Monyer H., '**Impaired electrical signaling disrupts gamma frequency oscillations in connexin 36-deficient mice**', Neuron. 2001 Aug 16;31(3):487-95
[http://dx.doi.org/10.1016/S0896-6273\(01\)00387-7](http://dx.doi.org/10.1016/S0896-6273(01)00387-7)

- [29] Litvin O., Tiunova A., Connell-Alberts Y., Panchin Y., Baranova A., **'What is hidden in the pannexin treasure trove: the sneak peek and the guesswork'**, J Cell. Mol. Med. 2006 Jul-Sep;10(3):613-34
<http://dx.doi.org/10.2755/jcmm010.003.04>
- [30] Alvarez V.A., Chow C.C., Bockstaele E.J.V., Williams J.T., **'Frequency-dependent synchrony in locus ceruleus: Role of electrotonic coupling'**, PNAS, Mar 2002; 99: 4032 - 4036.
<http://dx.doi.org/10.1073/pnas.062716299>
- [31] Shao J., Wright G.T., **'Characteristics of the Space-Charge-Limited Dielectric Diode at Very High Frequencies'**, Solid-State Elec., 1961, 3, pp. 291.
- [32] Martens H.C.F., Huiberts J.N., Blom P.W.M., **'Simultaneous measurement of electron and hole mobilities in polymer light-emitting diodes'**, App. Phys. Let. 77(12), 2000, pp. 1852-1854
<http://dx.doi.org/10.1063/1.1311599>
- [33] אפשטיין א., גולגר ל., 'אפיון תגובת התדר של דיודה פולטת אור מחומרים אורגניים', טכניון, חיפה, אוגוסט 2003.
<http://techst02.technion.ac.il/~sheket/p/1.pdf>
- [34] Bloodgood B.L., Sabatini B.L., **'Neuronal activity regulates diffusion across the neck of dendritic spines'**, Science. 2005 Nov 4;310(5749):866-9
<http://dx.doi.org/10.1126/science.1114816>
- [35] Benavides-Piccione R., Ballesteros-Yanez I., DeFelipe J., Yuste R., **'Cortical area and species differences in dendritic spine morphology'**, J Neurocytol. 2002 Mar-Jun;31(3-5):337-46
<http://dx.doi.org/10.1023/A:1024134312173>
- [36] Fukuda T., Kosaka T., Singer W., Galuske R.A., **'Gap junctions among dendrites of cortical GABAergic neurons establish a dense and widespread intercolumnar network'**, J Neurosci. 2006 Mar 29;26(13):3434-43
<http://dx.doi.org/10.1523/JNEUROSCI.4076-05.2006>
- [37] Araya R., Eisenthal KB, Yuste R., **'Dendritic spines linearize the summation of excitatory potentials'**, PNAS 2006 Dec 5;103(49):18799-804
<http://dx.doi.org/10.1073/pnas.0609225103>
- [38] Rose C.R., Konnerth A., **'NMDA receptor-mediated Na⁺ signals in spines and dendrites'**, J Neurosci. 2001 Jun 15;21(12):4207-14
<http://www.jneurosci.org/cgi/content/abstract/21/12/4207>
- [39] Gibson J.R., Beierlein M., Connors B.W., **'Functional Properties of Electrical Synapses Between Inhibitory Interneurons of Neocortical Layer 4'**, J Neurophysiol. 2003 Nov;90(5):2987-3000.
<http://dx.doi.org/10.1152/jn.00520.2004>
- [40] Srinivas M., Rozental R., Kojima T., Dermietzel R., Mehler M., Condorelli D.F., Kessler J.A., Spray D.C., **'Functional properties of channels formed by the neuronal gap junction protein connexin36'**, J Neurosci. 1999 Nov 15;19(22):9848-55
<http://www.jneurosci.org/cgi/content/abstract/19/22/9848>
- [41] Bruzzone R., Hormuzdi S.G., Barbe M.T., Herb A., Monyer H., **'Pannexins, a family of gap junction proteins expressed in brain'**, PNAS 2003 Nov 11;100(23):13644-9
<http://dx.doi.org/10.1073/pnas.2233464100>
- [42] Nitsche JM, Chang HC, Weber PA, Nicholson B.J., **'A transient diffusion model yields unitary gap junctional permeabilities from images of cell-to-cell fluorescent dye transfer between Xenopus oocytes'**, Biophys J. 2004 Apr;86(4):2058-77
<http://www.biophysj.org/cgi/content/abstract/86/4/2058>
- [43] Ashby M.C., Maier S.R., Nishimune A., Henley J.M., **'Lateral Diffusion Drives Constitutive Exchange of AMPA Receptors at Dendritic Spines and Is Regulated by Spine Morphology'**, J Neurosci. 2006 Jun 28;26(26):7046-55.
<http://www.jneurosci.org/cgi/content/abstract/26/26/7046>

- [44] Hille B., **'Ionic channels of excitable membranes'**, 2nd edn., Sinauer Associates, 1992.
- [45] Uhlhaas PJ, Singer W., **'Neural synchrony in brain disorders: relevance for cognitive dysfunctions and pathophysiology'**, *Neuron*. 2006 Oct 5;52(1):155-68
<http://dx.doi.org/10.1016/j.neuron.2006.09.020>
- [46] Fiala J.C., Spacek J., Harris K.M., **'Dendritic spine pathology: cause or consequence of neurological disorders?'**, *Brain Res Brain Res Rev*. 2002 Jun;39(1):29-54
[http://dx.doi.org/10.1016/S0165-0173\(02\)00158-3](http://dx.doi.org/10.1016/S0165-0173(02)00158-3)
- [47] Long M.A., Landisman C.E., Connors B.W., **'Small Clusters of Electrically Coupled Neurons Generate Synchronous Rhythms in the Thalamic Reticular Nucleus'**, *J. Neurosci.*, Jan 2004; 24: 341 - 349.
<http://dx.doi.org/10.1523/JNEUROSCI.3358-03.2004>
- [48] Pinto D.J., Jones S.R., Kaper T.J., Kopell N., **'Analysis of State-Dependent Transitions in Frequency and Long-Distance Coordination in a Model Oscillatory Cortical Circuit'**, *J. Comp. Neurosci.*, 15(2), Sep 2003, pp. 283 – 298
<http://dx.doi.org/10.1023/A:1025825102620>